Statistical Scaling of Geometric Characteristics in Millimeter Scale Natural Porous Media

A. Guadagnini · M. J. Blunt · M. Riva · B. Bijeljic

Received: 22 July 2013 / Accepted: 15 November 2013 / Published online: 30 November 2013

A. Guadagnini (✉) · M. J. Blunt · M. Riva
Dipartimento di Ingegneria Civile e Ambientale,
Politecnico di Milano, Piazza L. Da Vinci 32, 20133 Milano, Italy
e-mail: alberto.guadagnini@polimi.it

A. Guadagnini · M. Riva
Department of Hydrology and Water Resources,
University of Arizona, Tucson, AZ 85721, USA

M. J. Blunt · B. Bijeljic
Department of Earth Science and Engineering,
Imperial College, London, SW7 2AZ, UK

1 Introduction

The characterization of the pore-scale structure of natural and reconstructed porous media is the subject of intense research in several fields, including groundwater hydrology, oil and gas applications, geophysics, material science, and physics. Amongst different techniques which are employed to represent pore spaces, multiple-point statistics starting from two-dimensional thin sections have been employed to provide reconstructions of the three-dimensional pore space of millimeter scale rock samples which honor given statistics, typically in terms of variogram functions, within a prescribed observation window (e.g., Okabe and Blunt 2004, 2005, 2007, and references therein). Fractal models (see, e.g., Feder 1988 for early applica-tions of fractal concepts to porous media) of pore-space geometry have also been employed to discuss the fractal dimension of porosity of rock cores (e.g., amongst others Feder 1988; Sahimi and Yortsos 1991; Adler 1992; Pape et al. 1999). An overview of geometrical and stochastic characterization models for reconstruction of porous media is presented by Hil-fer (2002), to which the interested reader is referred. The author points out the relevance of considering multiple geometric observables to properly describe the system. Amongst these observables, the Minkowski functionals which are typically known as porosity (ϕ) and specific surface area (SSA) play a key role in classic continuum scale applications of flow and transport in porous media. These functionals were, for instance, employed by Latief et al. (2010) to provide quantitative comparisons between the results of a set of geometrical reconstruction techniques and microstructructural attributes of a centimeter scale block of Fontainbleau sandstone. Only limited insights are provided in the literature about the way statistics of these quantities are transferred across separation distances (lags) within a defined observation window and for the resolution typically achieved for images of rock samples.

The use of X-ray imaging has transformed our ability to quantify the pore structure of rock at the micron to millimeter scales (Wildenschild and Sheppard 2013; Blunt et al. 2013). In this paper, we use micron-resolution X-ray images to analyze two different rock samples. In this context, we focus on (a) documenting the possibility that porous media attributes such as ϕ and SSA directly measured at the pore scale display scaling of key statistics in a way which is consistent with the behavior displayed by many earth, environmental, biological, financial, and astrophysical quantities and described, e.g., in Neuman et al. (2013, and references therein); and (b) exploring the nature (e.g., fractal or multifractal) of such scaling. Our work thus complements classical results of analyses of these quantities at the millimeter observation scale and provides further elements for the characterization of the system evolution across different separation scales.

Neuman and Di Federico (2003) illustrate and document different types of scale dependencies of hydrogeological soil and rock properties. Scaling of statistics of sedimentary and fractured rock parameters have been reported, amongst others, by Molz and Boman (1995), Molz et al. (1997), Deshpande et al. (1997), Tennekoon et al. (2003), Castle et al. (2004), Guadagnini et al. (2012), Siena et al. (2012), and Riva et al. (2013a,b). All these studies are focused on the analysis of field (decameter) or laboratory (decimeter/meter) scale hydraulic conductivity/permeability data, the latter being associated with millimeter to meter scale measurement volumes. A number of studies are concerned with the analysis of the (fractal) scaling behavior of porous media attributes such as bulk density or particle and pore size distributions and geometry (see, e.g., Perfect and Kay 1995 for a review).

Paz Ferreiro et al. (2009) present a multifractal analysis of nitrogen adsorption isotherms obtained on centimeter scale samples of two agricultural soils. These authors observe that the multifractal parameters obtained vary markedly between soil types and highlight the potential usefulness of the observed scaling behavior to identify variations of specific surface area due to different soil management practices. Paz Ferreiro et al. (2010) describe scaling properties of mercury injection curves and nitrogen adsorption isotherms which are respectively employed to infer soil particle size distributions and SSA of millimeter scale agricultural soil aggregates. In these studies porosity and SSA are not measured directly from the knowledge of the micro-scale structure of the porous medium but are inferred from target state variables such as, for example, volume of absorbate or capillary pressure curves. As such, they are not geometrical observables in the sense of Hilfer (2002). Multifractal spectra of two-dimensional binary microtomographic images of millimeter scale soil aggregates were assessed by Kravchenko et al. (2009) to characterize the spatial distribution of pores. These authors noted that fractal scaling was potentially possible across a relatively narrow range of length scales and was limited by the presence of boundary conditions, an effect that is similar to the consequences of the cutoff scales introduced by Di Federico and Neuman (1997).

Here, we present a detailed analysis of the characterization of the scale statistics of porosity and specific surface area of millimeter scale samples of natural porous media. We consider two pore-scale rock samples, an Estaillades limestone and a Bentheimer sandstone. Both materials are standard quarry stones which have been employed as reproducible benchmarks for the study of flow and transport at the pore scale (Blunt et al. 2013; Bijeljic et al. 2013a,b). The micro-scale structure of each sample is reconstructed via X-ray micro-tomography with micrometer resolution. Scale dependence of statistics of incremental values of porosity and SSA are analyzed through the method of moments and extended self-similarity, following the works of Guadagnini et al. (2012), Siena et al. (2012), Neuman et al. (2013), and Riva et al. (2013a,b).

2 Experimental Data-Sets and Theoretical Basis

We study samples of two different (natural) rocks. Bentheimer sandstone is a quartz-rich quarry sandstone with a well-connected pore space. It is mainly used in buildings, including the pedestal of the Statue of Liberty in New York. Estaillades carbonate is composed of small calcite grains and is characterized by a highly irregular pore space with micro-porosity that cannot be resolved with micro-CT scanning (Bijeljic et al. 2013b). The three-dimensional structure of each sample has been reconstructed via X-ray micro-tomography using a bench-top scanner (Xradia Versa 500) with spatial resolution of $d = 3.0$ and $3.3\,\mu$m, respectively, for the sandstone and limestone blocks. From the core of each rock samples we extract an array of 300^3 or 650^3 voxels, resulting in an overall characteristic length of the analyzed blocks of $l = 0.9$ and 2.14 mm, respectively, for the sandstone and limestone samples. The raw scans were filtered using a non-local means edge preserving filter to reduce noise (Buades et al. 2005, 2008). The images were then segmented into pore and grain regions using a seeded watershed algorithm based on the three-dimensional gradient magnitude and grey-scale value of each voxel. This eliminates much of the voxel misidentification which can occur in simple grey-scale segmentation, as well as the arbitrary nature of the thresholds taken. It also eliminates partial volume artefacts. All image processing was conducted within the Avizo Fire 7.0 program (VSG; www.vsg3d.com). Porosity is the fraction of the voxels that are void. SSA is the area of the interface between pore and grain voxels, per unit volume.

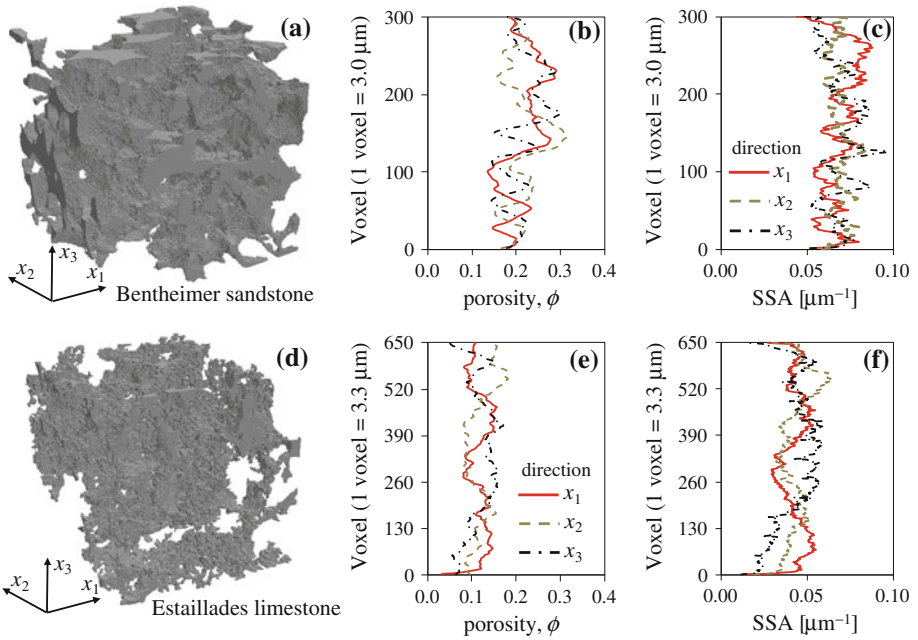

Fig. 1 Images of pore space structure, directional distribution of porosity, and SSA for **a–c** Bentheimer sandstone, and **d–f** Estaillades limestone

Figure 1 depicts images of the samples together with extracted directional distributions of porosity, ϕ, and specific surface area, SSA. The distributions of porosity, ϕ, and SSA along the three mutually orthogonal directions x_i (i = 1, 2, 3) represented in Fig. 1 and associated with rock volumes of size $d \times l^2$ are calculated by applying the methodology of Coker and Torquato (1995) to the digitized binary images.

We investigate power-law scaling of order q sample structure functions of absolute increments, defined as

$$S_N^q(s_i) = \frac{1}{N(s_i)} \sum_{n=1}^{N(s)} |\Delta y_n(s_i)|^q \tag{1}$$

$y(x)$ being a sample of a random field $Y(x)$ defined on a continuum of points x in a one-dimensional setting and representing either ϕ or SSA. Here, $\Delta y_n(s_i) = y(x_{i,n} + s_i) - y(x_{i,n})$ is an increment of $y(x_i)$ calculated over a lag (separation distance) s_i between two points along direction x_i and $N(s_i)$ is the number of such increments. Power-law scaling which has been observed for a variety of physical, geophysical, ecological, environmental, biological, and financial variables is defined as

$$S_N^q(s_i) \propto s_i^{\xi_i(q)} \tag{2}$$

where the power or scaling exponent, $\xi_i(q)$, can vary with direction x_i and is independent of s_i.

We identify and analyze the occurrence of directional power-law scaling for incremental values of ϕ or SSA calculated along the three directions x_i (i = 1, 2, 3) of Fig. 1 through the method of moments (M) and extended self-similarity (ESS).

Within the context of the method of moments, sample structure functions (1) are inferred for a set of separation lags and a series, $q_1, q_2, \ldots, q_n$, of q values. The structure function $S_N^{q_j}$ is plotted against s_i on a log–log scale and the power $\xi_\mathrm{i}(q_j)(j = 1, 2, ..., n)$ is calculated as the slope of the resulting linear regression line. A linear or near-linear dependence of log $S_N^{q_j}$ on log s_i is usually obtained within intermediate ranges of lags, $s_I < s_\mathrm{i} < s_{II}$, s_I and s_{II} being defined theoretically or, in most cases, empirically (Stumpf and Porter 2012; Siena et al. 2012 and references therein).

ESS is an empirical procedure introduced by Benzi et al. (1993a,b). It enables one to extend power-law scaling at all separation scales and is based on the observation that

$$S_N^n(s_\mathrm{i}) \propto S_N^m(s_\mathrm{i})^{\beta_\mathrm{i}(n,m)} \tag{3}$$

Here, $\beta_\mathrm{i}(n, m) = \xi_\mathrm{i}(n)/\xi_\mathrm{i}(m)$ is the ratio between the scaling exponents of S_N^n and S_N^m. Application of ESS to enlarge scaling ranges and obtain a corresponding improvement in the accuracy of $\xi_\mathrm{i}(q)$ estimates has been illustrated empirically for various data, including turbulent velocities, geographical, hydraulic, atmospheric, astrophysical, biological, financial time series, and ecological variables (Nikora and Goring 2001; Guadagnini and Neuman 2011; Leonardis et al. 2012, and references therein).

When the scaling exponent is linearly proportional to q, $\xi(q) = Hq$, $Y(x)$ is typically interpreted as a self-affine random field (or process) with Hurst exponent H. When $\xi(q)$ displays nonlinear dependence on q, $Y(x)$ has typically been interpreted as a multifractal process (e.g., Sahimi and Yortsos 1991; see also a recent literature review by Neuman et al. 2013) or, more recently, as fractional Laplace motion (Meerschaert et al. 2004). Nonlinear behavior of $\xi(q)$ has been shown theoretically and numerically by Neuman (2010a,b, 2011), Siena et al. (2012), Neuman et al. (2013), and Riva et al. (2013a) to be associated with square or absolute increments of samples collected from (a) truncated fractional Brownian motion (tfBm) and (b) sub-Gaussian processes subordinated to tfBm with heavy tailed subordinators such as log-normal or Lévy at intermediate ranges of lags and may be the mark of apparent multifractality. These authors further suggest that the behavior displayed by many environmental and geophysical variables, including manifestations of: (a) nonlinear power-law scaling of sample structure functions in a midrange of lags, with breakdown in such scaling at small and large lags; (b) extended power-law scaling at all lags; (c) nonlinear scaling of power-law exponent with order of sample structure function; and (d) pronounced statistical anisotropy is consistent with a novel interpretation that views such variables as samples from stationary, anisotropic sub-Gaussian random fields or processes subordinated to tfBm or truncated fractional Gaussian noise (tfGn). These quantities are thus modeled as mixtures of Gaussian components having random variances (see, e.g., Samorodnitsky and Taqqu 1994; Neuman et al. 2013). As proposed by Di Federico and Neuman (1997) and Di Federico et al. (1999) and illustrated by Neuman and Di Federico (2003) and Neuman et al. (2013), tfBm and tfGn, respectively, arise from truncation of (monofractal) fBm and fGn which is performed by filtering out components below the measurement/resolution scale and above the scale of data sampling domain. Guadagnini et al. (2012), Guadagnini et al. (2014), Siena et al. (2012), and Riva et al. (2013a,b) demonstrate the consistency of such novel approach of geostatistical inference with a variety of laboratory and field scale hydraulic and soil texture data from sedimentary and fractured rocks.

A theoretical basis for ESS has been proposed by Chakraborty et al. (2010) with reference to the one-dimensional Burger's equation. Siena et al. (2012) show that ESS is consistent with (Gaussian) tfBm. Neuman et al. (2013) provide a theoretical basis to the behavior encapsulated in ESS-based empirical evidences by proving that ESS is consistent, at all separation scales, with the type of random processes described above.

3 Directional Scaling of Porosity and Specific Surface Increments

Increments of ϕ and SSA are calculated for lags $s_i \leq 150$ or 325 voxels (yielding a number of directional increment samples varying from 299 to 150 or 649 to 325), respectively, for the sandstone and limestone media, to assure that a sufficient number of samples can be employed for the estimation of q order structure functions. The number of samples is not sufficient to obtain meaningful structure function estimates for $q > 4$.

Figure 2 illustrates the type of dependence observed for increments of ϕ parallel to x_1 for the two rock samples investigated. Figure 3 presents the corresponding depiction associated with SSA. The range $s_{1,I} < s_1 < s_{1,II}$ within which power-law scaling can be recognized is delineated by dashed vertical lines. These ranges are generally narrower for the sandstone than for the limestone, respectively extending over one and two decades. They are seen to be typically larger for SSA than for ϕ and are not affected by direction (not shown).

The method of moments (M) relies on plotting $\log S_N^{q_j}$ for $j = 1, 2, ..., n$ versus $\log s_i$ and linearly relating the former to the latter within the range $s_{i,I} < s_i < s_{i,II}$. Directional scaling exponents $\xi_i(q)$ are then estimated from the slope of the corresponding regression line. We estimated $\xi_i(q)$ by varying the lower and upper lag values, $s_{i,I}$ and $s_{i,II}$, delimiting

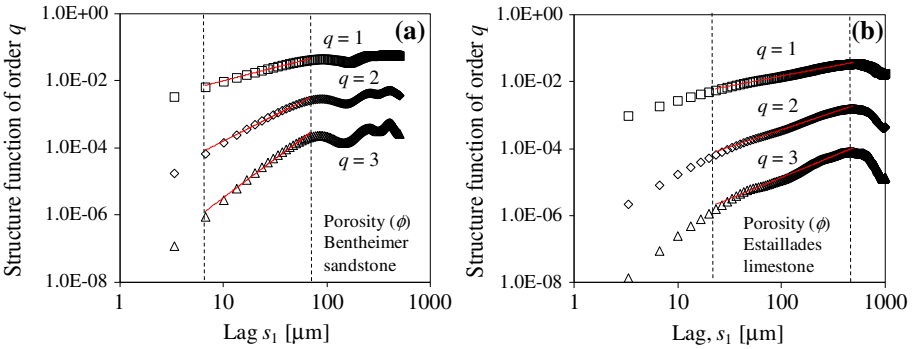

Fig. 2 Dependence of sample structure functions of order q =1, 2, 3 of absolute increments of porosity on lag along x_1 axis (Fig. 1), s_1, for **a** Bentheimer sandstone, and **b** Estaillades limestone. *Dashed vertical lines* demarcate the range within which power-law scaling can be indentified

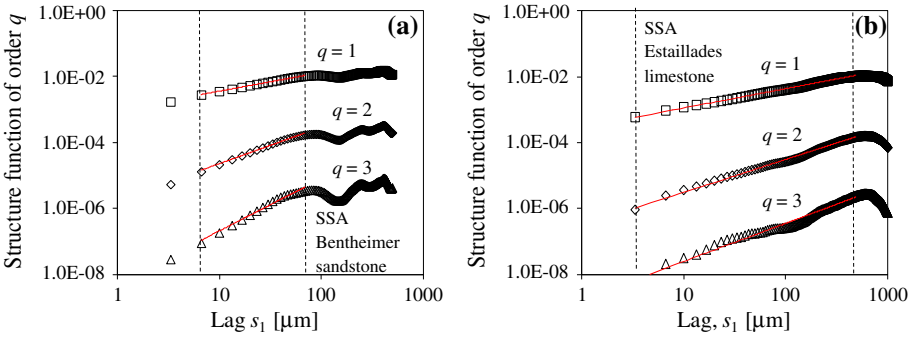

Fig. 3 Dependence of sample structure functions of order q =1, 2, 3 of absolute increments of SSA on lag along x_1 axis, s_1, for **a** Bentheimer sandstone, and **b** Estaillades limestone. *Dashed vertical lines* demarcate the range within which power-law scaling can be identified

the power law scaling range and selecting that pair of lags which yields the largest R^2. Our results imply that, in a midrange of lags, each structure function scales as a power of lag. Application of M to increments in the x_i (i = 1, 2, 3) directions on each rock sample for $0.1 \leq q \leq 4.0$ yields regression lines with coefficients of determination, R^2, which are always larger than 0.97.

Figure 4 depicts examples of the dependence of $\log S_N^{q+1}$ on $\log S_N^q$ based on the application of ESS to the incremental data of SSA computed along direction x_1 over the two rock samples. Similar behavior is observed for all cases analyzed, revealing that S_N^q exhibits extended power-law scaling at all lags. Coefficients of determination (R^2) associated with regression lines fitted to the curves in Fig. 4 are seen to be always 0.99–1.00.

The method of moments and ESS are then employed to compute directional values of $\xi_i(q)$. Application of ESS relies on (*a*) computing $\beta_i(q + \Delta q, q) = \xi_i(q + \Delta q)/\xi_i(q)$ for given Δq; (*b*) computing a reference value, $\xi_{i,ref}$, of $\xi_i(q)$ for a selected $q = q_{\text{ref}}$ by M; and (*c*) starting from $\xi_{i,\text{ref}}$ to evaluate $\xi_i(q + \Delta q)$ and $\xi_i(q - \Delta q)$ according to step (*a*). As did Guadagnini et al. (2012), we use $\xi_{i,\text{ref}} = \xi_i(1)$ for all variables and directions, to account for possible deterioration of accuracy in estimating structure functions with increasing q.

Figure 5 plots variations of $\xi_i(q)$ with q for ϕ computed through ESS upon setting $\Delta q = 0.1$ for $0.1 \leq q \leq 1.0$ and $\Delta q = 0.5$ for $1.0 < q \leq 4.0$ along the three directions

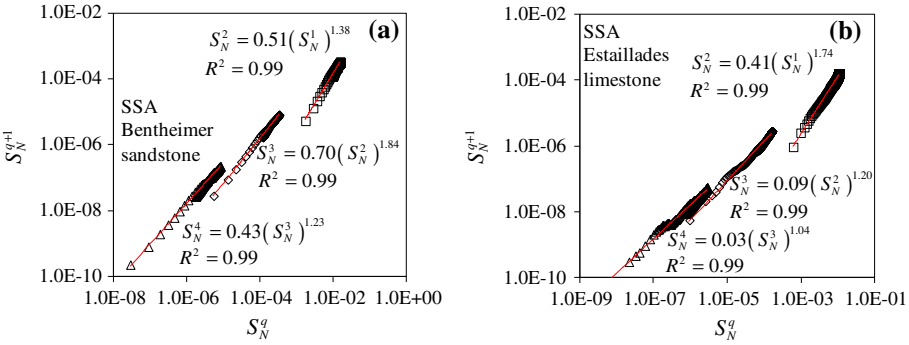

Fig. 4 Dependence of S_N^{q+1} on S_N^q for integer q= 1–3 and increments of SSA parallel to x_1 axis on **a** Bentheimer sandstone, and **b** Estaillades limestone. Linear regression equations and associated coefficients of determination (R^2) are included

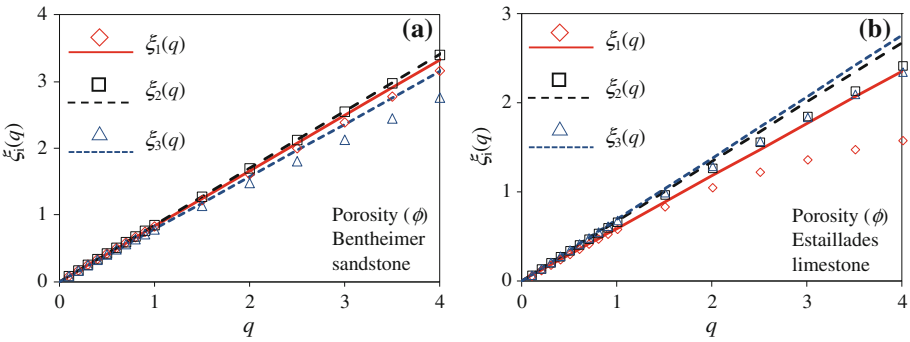

Fig. 5 Directional dependence of $\xi_i(q)$ (i = 1, 2, 3) on q obtained through ESS for increments of porosity along x_1 (*red diamonds*), x_2 (*black squares*), and x_3 (*blue triangles*) axis on **a** Bentheimer sandstone, and **b** Estaillades limestone. *Straight lines* have slopes equal to those of $\xi_i(q = 1)$

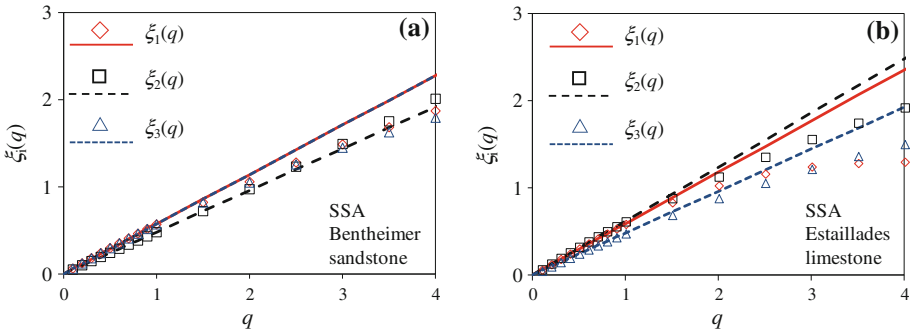

Fig. 6 Directional dependence of $\xi_i(q)$ (i = 1, 2, 3) on q obtained through ESS for increments of SSA along x_1 (*red diamonds*), x_2 (*black squares*), and x_3 (*blue triangles*) axis on **a** Bentheimer sandstone, and **b** Estaillades limestone. *Straight lines* have slopes equal to those of $\xi_i(q = 1)$

Table 1 Estimates $\hat{H}$ based on the method of moments applied to directional increments of ϕ and SSA of Bentheimer sandstone and Estaillades limestone

	$\hat{H}$ associated with ϕ			$\hat{H}$ associated with SSA		
Direction	x_1	x_2	x_3	x_1	x_2	x_3
Bentheimer sandstone	0.83	0.85	0.78	0.57	0.48	0.57
Estaillades limestone	0.59	0.67	0.69	0.58	0.62	0.48

represented in Fig. 1. The method of moments yields very similar results. Figure 6 reports the corresponding depiction for SSA. Each figure includes straight lines associated with a slope equal to that of $\xi_i(q = 1)$. The latter is typically interpreted as an estimate of the Hurst exponent associated with the degree of (spatial) persistence of the signal.

Figures 5 and 6 reveal that the power $\xi_i(q)$ tends to be quasi-linear in q for ϕ and SSA of the sandstone sample. On the other hand, both ϕ and SSA associated with the limestone sample are markedly nonlinear concave in q for all increment orientations in the directions analyzed. We note that there is an apparent anisotropic behavior of $\xi_i(q)$. Such behavior appears to be mild for the sandstone sample while it is marked for both porosity and SSA of the limestone. Additional investigations on different blocks of the same rock matrices (eventually associated with different sizes and different image resolutions) and/or different types of media are required to completely characterize this behavior and possibly link it to evolutionary/depositional processes affecting the pore-space geometry.

Table 1 collects estimated values $\hat{H}$ of H associated with the detected directional power-law scaling of ϕ and SSA. Our results show that both variables generally display mild to strong persistent behavior, varying in a smooth rather than a rough fashion as was the case in Fig. 1. The observed persistent behavior of ϕ is consistent with estimates of the Hurst exponent obtained by Dashtian et al. (2011) who analyzed neutron porosities of well logs from three reservoirs with geology ranging from shaly sands to fractured carbonate and estimated values of $H > 0.8$. However, no studies of the kind we present at a similar scale are available for a direct comparison.

Whereas the literature attributes nonlinear scaling of $\xi_i(q)$ with q to multifractal fields or to fractional Laplace motion, we find the observed nonlinearity to be consistent with sub-Gaussian random fields subordinated to tfBm (or tfGn), in agreement with the theoretical, numerical and experimental evidences of Neuman (2010a,b, 2011), Neuman et al. (2013),

Siena et al. (2012), Guadagnini and Neuman (2011), Guadagnini et al. (2012, 2014) and Riva et al. (2013a,b).

4 Conclusions

Our work leads to the following major conclusions:

1. Order q sample structure functions of absolute porosity (ϕ) and specific surface area (SSA) increments calculated on digitized images (with micro-meter resolution) of three-dimensional millimeter scale samples of a sandstone and a limestone rock scale as a power $\xi_i(q)$ of directional lag, s_i, over a range of lags extending at least one decade within the observation window associated with the size of the porous medium. Extended power-law scaling, revealed through extended self similarity (ESS), appears to be an intrinsic property of the quantities analyzed for both media at the investigated scale.
2. Moment and extended self-similarity methods reveal that $\xi_i(q)$ for both ϕ and SSA tends to be quasi-linear or nonlinear in q, respectively, for the sandstone and limestone blocks. This could be a consequence of the increased complexity of the internal organization of the void space in the limestone as opposed to the sandstone medium. Although further studies are required to test our findings on additional samples and to assess the impact of image resolution, these results are in line with the observation that the limestone is more heterogeneous in structure, flow and transport. This is shown, e.g., by numerical simulations performed through these images (Blunt et al. 2013; Bijeljic et al. 2013a,b) which demonstrate that carbonate (limestone) rocks display a wider range of local flow velocities at the pore scale giving rise to a qualitatively different nature of transport with highly anomalous long tailing in comparison to the sandstone.
3. Although the literature commonly attributes the type of nonlinear scaling we document to multifractals and/or fractional Laplace motions, our results are fully consistent with the behavior displayed by samples from sub-Gaussian random fields subordinated to truncated fractional Brownian motion or Gaussian noise which predict theoretically the observed breakdown in power-lag scaling at short and large lags and ESS behavior. Both porosity and SSA display mild to strongly persistent behavior, with estimates $\hat{H}$ generally depending on direction. Additional investigations on different media (eventually associated with different sizes and different image resolutions) are required to completely characterize this behavior and possibly link it to evolutionary/depositional processes affecting the pore-space geometry.

Acknowledgments Funding from MIUR (Italian Ministry of Education, Universities and Research-PRIN2010-11; project: "Innovative methods for water resources under hydro-climatic uncertainty scenarios") is acknowledged. The authors are grateful to M. Siena for providing the algorithm and code for the extraction of porosity and SSA from the digitized binary images. The authors thank S.P. Neuman for stimulating discussions.

References

Adler, P.M.: Porous Media: Geometry and Transports. Butterworth-Heinemann, Boston (1992)

Benzi, R., Ciliberto, S., Baudet, C., Chavarria, G.R., Tripiccione, R.: Extended self-similarity in the dissipation range of fully developed turbulence. Europhys. Lett. **24**, 275–279 (1993a). doi:10.1209/0295-5075/24/4/007

Benzi, R., Ciliberto, S., Tripiccione, R., Baudet, C., Massaioli, F., Succi, S.: Extended self-similarity in turbulent flows. Phys. Rev. E **48**, R29–R32 (1993b). doi:10.1103/PhysRevE.48.R29
Bijeljic, B., Raeini, A., Mostaghimi, P., Blunt, M.J.: Predictions of non-Fickian solute transport in different classes of porous media using direct simulation on pore-scale images. Phys. Rev. E. **87**, 013011 (2013a). doi:10.1103/PhysRevE.87.013011
Bijeljic, B., Mostaghimi, P., Blunt, M.J.: Insights into non-Fickian solute transport in carbonates. Water Resour. Res. **49**(5), 2714–2728 (2013b). doi:10.1002/wrcr.20238
Blunt, M.J., Bijeljic, B., Dong, H., Gharbi, O., Iglauer, S., Mostaghimi, P., Paluszny, A., Pentland, C.: Pore-scale imaging and modelling. Adv. Water Resour. **51**, 197–216 (2013)
Buades, A., Coll, B., Morel, J.-M.: A non-local algorithm for image denoising. CVPR '05 Proceedings of the 2005 IEEE Computer Society Conference on Computer Vision and Pattern Recognition (CVPR'05) 2, pp. 60–65, 2005
Buades, A., Coll, B., Morel, J.-M.: Nonlocal image and movie denoising. Int. J. Comput. Vision **76**, 123–139 (2008)
Castle, J.W., Molz, F.J., Lu, S., Dinwiddie, C.L.: Sedimentology and fractal-based analysis of permeability data, John Henry member, Straight Cliffs formation (upper Cretaceous), Utah, U.S.A. J. Sediment. Res. **74**(2), 270–284 (2004)
Chakraborty, S., Frisch, U., Ray, S.S.: Extended self-similarity works for the Burgers equation and why. J. Fluid Mech. **649**, 275–285 (2010). doi:10.1017/S0022112010000595
Coker, D.A., Torquato, S.: Extraction of morphological quantities from a digitized medium. J. Appl. Phys. **77**(121), 6087–6099 (1995)
Dashtian, H., Jafari, G.R., Sahimi, M., Msihi, M.: Scaling, multifractality, and long-range correlations in well log data of large-scale porous media. Physica A **390**, 2096–2111 (2011). doi:10.1016/j.physa.2011.01.010
Deshpande, A., Flemings, P.B., Huang, J.: Quantifying lateral heterogeneities in fluvio-deltaic sediments using three-dimensional reflection seismic data: Offshore Gulf of Mexico. J. Geophys. Res. **102**(B7), 15385–15401 (1997)
Di Federico, V., Neuman, S.P.: Scaling of random fields by means of truncated power variograms and associated spectra. Water Resour. Res. **33**, 1075–1085 (1997). doi:10.1029/97WR00299
Di Federico, V., Neuman, S.P., Tartakovsky, D.M.: Anisotropy, lacunarity, upscaled conductivity and its covariance in multiscale fields with truncated power variograms. Water Resour. Res. **35**(10), 2891–2908 (1999)
Feder, J.: Fractals. Plenum Press, New York (1988)
Guadagnini, A., Neuman, S.P., Schaap, M.G., Riva, M.: Anisotropic Statistical Scaling of Soil and Sediment Texture in a Stratified Deep Vadose Zone near Maricopa, Arizona, Geoderma 214–215, 217–227 (2014). doi:10.1016/j.geoderma.2013.09.008
Guadagnini, A., Neuman, S.P.: Extended self-affinity of signals exhibiting apparent multifractality. Geophys. Res. Lett. **38**, L13403 (2011). doi:10.1029/2011GL047727
Guadagnini, A., Neuman, S.P., Riva, M.: Numerical investigation of apparent multifractality of samples from processes subordinated to truncated fBm. Hydrol. Process. **26**, 2894–2908 (2012). doi:10.1002/hyp.8358
Hilfer, R.: Review on scale dependent characterization of the microstructure of porous media. Transport Porous Med. **46**, 373–390 (2002)
Kravchenko, A.N., Martín, M.A., Smucker, A.J.M., Rivers, M.L.: Limitations in determining multifractal spectra from pore-solid soil aggregate images. Vadose Zone J. **8**, 220–226 (2009)
Latief, F.D.E., Biswal, B., Fauzi, U., Hilfer, R.: Continuum reconstruction of the pore scale microstructure for Fontainebleau sandstone. Physica A **389**, 1607–1618 (2010)
Leonardis, E., Chapman, S.C., Foullon, C.: Turbulent characteristics in the intensity fluctuations of a solar quiescent prominence observed by the Hinode Solar Optical Telescope. Astrophys. J. **745**, 185 (2012). doi:10.1088/0004-637X/745/2/185
Meerschaert, M.M., Kozubowski, T.J., Molz, F.J., Lu, S.: Fractional laplace model for hydraulic conductivity. Geophys. Res. Lett. **31**, L08501 (2004). doi:10.1029/2003GL019320
Molz, F., Boman, G.: Further evidence of fractal structure in hydraulic conductivity distributions. Geophys. Res. Lett. **22**(18), 2545–2548 (1995)
Molz, F., Liu, H., Szulga, J.: Fractional Brownian motion and fractional Gaussian noise in subsurface hydrology: a review, presentation of fundamental properties, and extensions. Water Resour. Res. **33**(10), 2273–2286 (1997)
Neuman, S.P., Di Federico, V.: Multifaceted nature of hydrogeologic scaling and its interpretation. Rev. Geophys. **41**(3), 1014 (2003). doi:10.1029/2003RG000130
Neuman, S.P.: Apparent/spurious multifractality of data sampled from fractional Brownian/Lévy motions. Hydrol. Process. **24**, 2056–2067 (2010a). doi:10.1002/hyp.7611
Neuman, S.P.: Apparent/spurious multifractality of absolute increments sampled from truncated fractional Gaussian/Lévy noise. Geophys. Res. Lett. **37**, L09403 (2010b). doi:10.1029/2010GL043314

Neuman, S.P.: Apparent multifractality and scale-dependent distribution of data sampled from self-affine processes. Hydrol. Process. **25**, 1837–1840 (2011). doi:10.1002/hyp.7967
Neuman, S.P., Guadagnini, A., Riva, M., Siena, M.: Recent advances in statistical and scaling analysis of earth and environmental variables. In: Mishra, P.K., Kuhlman, K.L. (eds.) Recent Advances in Hydrogeology, pp. 11–15. Springer Science+Business Media, New York (2013)
Nikora, V.I., Goring, D.G.: Extended self-similarity in geophysical and geological applications. Math. Geol. **33**(3), 251–271 (2001). doi:10.1023/A:1007630021716
Okabe, H., Blunt, M.J.: Prediction of permeability for porous media reconstructed using multiple-point statistics. Phys. Rev. E. **70**, 066135 (2004). doi:10.1103/PhysRevE.70.066135
Okabe, H., Blunt, M.J.: Pore space reconstruction using multiple-point statistics. J. Petrol. Sci. Eng. **46**, 121–137 (2005). doi:10.1016/j.petrol.2004.08.002
Okabe, H., Blunt, M.J.: Pore space reconstruction of vuggy carbonates using microtomography and multiple-point statistics. Water Resour. Res. **43**, W12S02 (2007). doi:10.1029/2006WR005680
Pape, H., Clauser, C., Iffland, J.: Permeability prediction based on fractal pore-space geometry. Geophysics **64**(5), 1447–1460 (1999)
Paz Ferreiro, J., Wilson, M., Vidal Vázquez, E.: Multifractal description of nitrogen adsorption isotherms. Vadose Zone J. **8**, 209–219 (2009)
Paz Ferreiro, J., Miranda, J.G.V., Vidal Vázquez, E.: Multifractal analysis of soil porosity based on mercury injection and nitrogen adsorption. Vadose Zone J. **9**(2), 325–335 (2010)
Perfect, E., Kay, B.D.: Applications of fractals in soil and tillage research: a review. Soil Tillage Res. **36**, 1–20 (1995)
Riva, M., Neuman, S.P., Guadagnini, A., Siena, M.: Anisotropic scaling of Berea sandstone log air permeability statistics. Vadose Zone J. **12**(3), (2013b). doi:10.2136/vzj2012.0153
Riva, M., Neuman, S.P., Guadagnini, A.: Sub-Gaussian model of processes with heavy tailed distributions applied to permeabilities of fractured tuff. Stoch. Environ. Res. Risk Assess. **27**, 195–207 (2013a). doi:10.1007/s00477-012-0576-y
Sahimi, M., Yortsos, Y.C.: Applications of fractal geometry to porous media: a review. SPE 20476, Society of Petroleum Engineers (1991)
Samorodnitsky, G., Taqqu, M.S.: Stable Non-Gaussian Random Processes. Chapman & Hall, New York (1994)
Siena, M., Guadagnini, A., Riva, M., Neuman, S.P.: Extended power-law scaling of air permeabilities measured on a block of tuff. Hydrol. Earth Syst. Sci. **16**, 29–42 (2012). doi:10.5194/hess-16-29-2012
Stumpf, M.P.H., Porter, M.A.: Critical truths about power laws. Science **335**, 665–666 (2012)
Tennekoon, L., Boufadel, M.C., Lavallee, D., Weaver, J.: Multifractal anisotropic scaling of the hydraulic conductivity. Water Resour. Res. **39**(7), 1193 (2003). doi:10.1029/2002WR001645
Wildenschild, D., Sheppard, A.P.: X-ray imaging and analysis techniques for quantifying pore-scale structure and processes in subsurface porous medium systems. Adv. Water Resour. **51**, 217–246 (2013)